

A theory for phase locking of respiration in cats to a mechanical ventilator

G. A. PETRILLO AND LEON GLASS

*Departments of Electrical Engineering and Physiology, McGill University,
Montreal, Quebec H3G 1Y6, Canada*

PETRILLO, G. A., AND LEON GLASS. *A theory for phase locking of respiration in cats to a mechanical ventilator*. *Am. J. Physiol.* 246 (Regulatory Integrative Comp. Physiol. 15): R311–R320, 1984.—A mathematical model describing the Hering-Breuer reflexes in mechanically ventilated cats is developed. There is good agreement between the properties of the model and experimental studies performed over a wide range of frequencies and volumes of the mechanical ventilator. There is a correspondence between the model and a periodically forced nonlinear oscillator, similar to the van der Pol equation. Brain stem mechanisms underlying the entrainment are discussed.

artificial ventilation; Hering-Breuer reflex; limit cycle oscillation; entrainment

A COMMON FEATURE of biological oscillators is their propensity to become entrained or phase locked to a periodically imposed input. In the phase-locked condition, there is an integral ratio between the imposed frequency and the frequency of the biological oscillator (commonly small integers), and the dynamics are periodic in time.

The intrinsic respiratory rhythm of mammals, which is generated in the brain stem, can be phase locked to a mechanical ventilator (1–3, 13, 15, 32, 34, 35, 41). It is believed that the main stimuli underlying the phase locking originate from stretch and pressure receptors in the lung and bronchial airways (32, 35, 41). The effect of lung inflation during inspiration is to shorten inspiratory time (Hering-Breuer inspiratory inhibitory reflex), whereas a lung inflation delivered during expiration lengthens expiratory time (Hering-Breuer expiratory-promoting reflex) (5). The Hering-Breuer reflexes are mediated by vagal afferent activity. Entrainment to a mechanical ventilator is lost by sectioning the vagus nerves (32, 35).

In a recent paper, we described the phase locking of the respiratory rhythm of paralyzed cats to a mechanical ventilator (35). Extensive data were reported on the entrainment over a large range of frequencies and amplitudes of the mechanical ventilator. In this paper we develop a mathematical model for this experimental system.

Mathematical models have been developed for the effects of single lung inflations delivered during the

respiratory cycle on the subsequent timing of the respiratory phases (4, 7, 10, 24, 27, 41, 43). These mathematical models should, in principle, also be capable of predicting the effects of periodic mechanical ventilation. Our goal in the following is to take the main ideas developed by von Euler and co-workers on the Hering-Breuer reflexes (4, 7, 27) and adopt them for the modeling of respiratory entrainment by periodic lung inflation. A similar approach is taken by Baconnier et al. (3). However, in contrast to the work of Baconnier et al. (3), we have tried to simplify the von Euler model as much as possible. The mathematical model we develop has 5 adjustable parameters, all of which have a simple physiological interpretation. The original von Euler model, as adopted by Baconnier et al. (3), has more than 10 parameters.

Two other complementary approaches have also been used previously to develop quantitative models for respiratory phase locking.

1) The effects of a single-pulse inflation on respiratory timing at different phases of the respiratory cycle are measured. These measurements are then used to predict the effects of periodic pulse inflations (2, 3, 41). These techniques have also been used to study periodic forcing of neural and cardiac pacemaker cells (23, 33, 39). For the techniques to be valid, the stimulus in the periodic train must be identical to the stimulus used in the single-pulse phase-resetting experiments. This criterion is generally not easy to satisfy in respiratory entrainment studies, since the length of inflation pulses is often varied to maintain constant CO_2 (41).

2) Nonlinear differential equations, such as the van der Pol oscillator, have been adopted as models for the central respiratory rhythm generator (2, 3, 15). The effects of mechanical ventilation are then represented by assuming a periodic forcing function as an input to the nonlinear oscillator. As we show in the APPENDIX, nonlinear equations of the van der Pol type are closely related to the model developed here for the control of respiration.

In section I we present a brief summary of experimental results from a previous paper. In section II we present the mathematical model for respiratory phase locking and determine the parameters in the model. The properties of the model, found from numerical simulation, are presented in section III. The results are discussed in section IV.

I. EXPERIMENTAL RESULTS

The following is a brief summary of experimental results that are reported in detail elsewhere (34, 35). Experiments were performed on anesthetized, paralyzed adult cats, mechanically ventilated with a modified Harvard ventilator. End-tidal CO_2 and O_2 were maintained constant by modifying the breathing gas mixture at different ventilator volumes and frequencies.

Altering the frequency and volume of the ventilator

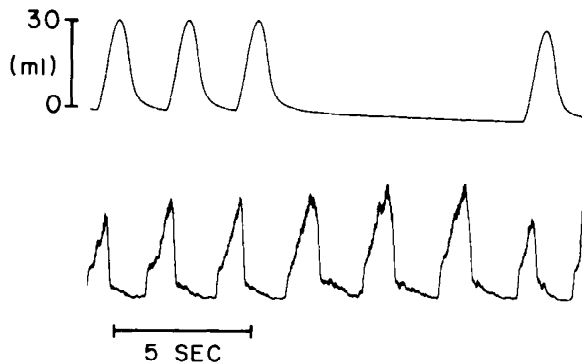


FIG. 1. Lung volume delivered by mechanical ventilator and corresponding "integrated" phrenic activity found by passing phrenic signal through filter with time constant of 100 ms (35). When ventilator is turned off, periodic phrenic bursts continue giving $T_I = 1.0$ s and $T_E = 2.0$ s.

produces a variety of different patterns between the mechanical ventilator and the phrenic activity. Figure 1 shows a trace from a typical experiment. The top line shows the volume delivered by the mechanical ventilator, and the bottom line shows the "integrated" phrenic activity. At first there is 1:1 phase locking (or entrainment) in which for each ventilator cycle there is one phrenic burst coming at the same phase of the ventilator cycle. After three cycles of 1:1 entrainment, the ventilator was turned off. The phrenic bursts continue, even in the absence of periodic input. The phrenic bursts with the ventilator turned off were used to determine the intrinsic inspiratory time (T_I), and the intrinsic expiratory time (T_E). Figure 2 shows a composite plot of the boundaries of the different phase-locking regions and traces of the patterns in the different regions. The boundaries between the different regions vary from cat to cat, but the different phase-locking zones can generally be observed in each cat, provided the appropriate amplitude and volume of the ventilator are selected.

In Figs. 3 and 4 we show several important features of phase locking in the 1:1 zone in one cat. Figure 3A shows the expiratory and inspiratory times (T_E and T_I , respectively) as measured from "integrated" phrenic activity. The values of T_I and T_E vary so that $f = 1/(T_I + T_E)$, where f is the ventilator frequency (35). In the 1:1 zone as the frequency and volume change there is a change in

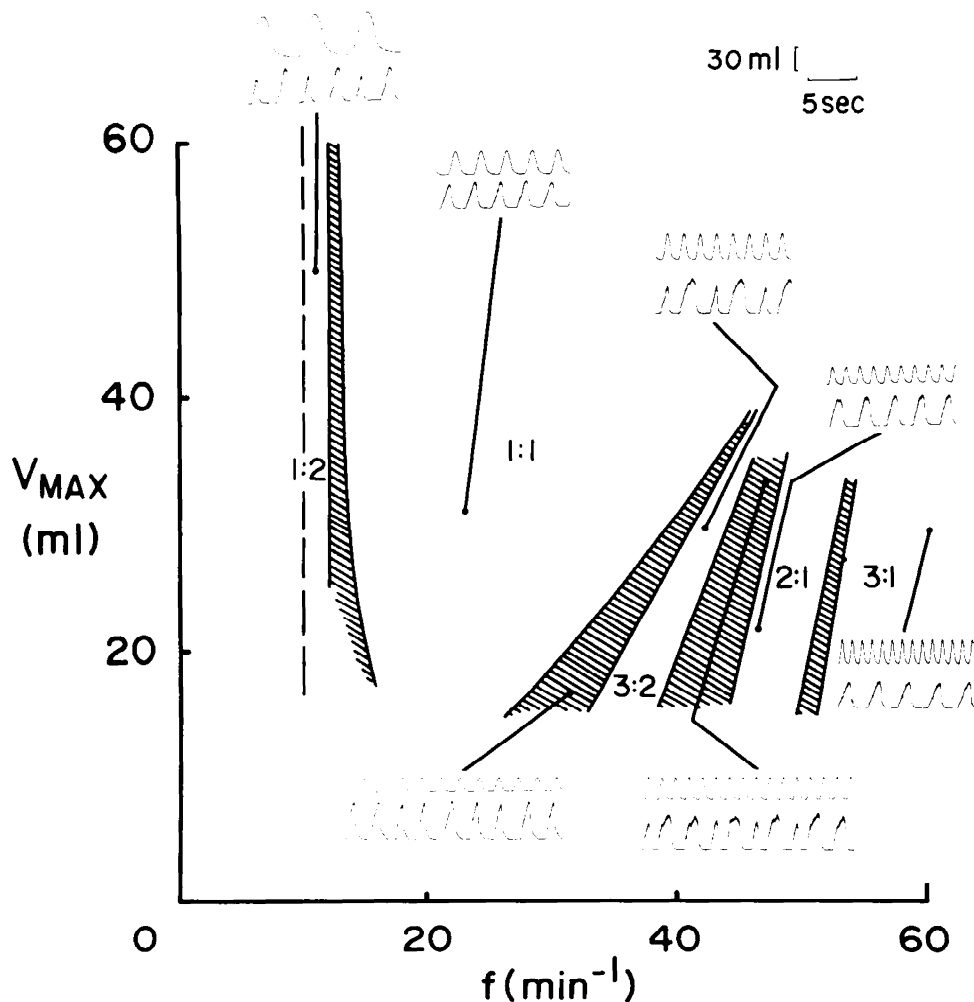


FIG. 2. Composite showing schematic diagram of different phase-locking zones obtained experimentally and representative traces of dynamics in each zone. In each inset, upper trace is lung volume, and lower trace is "integrated" phrenic activity. Scale is the same for all insets. In regions between stable phase-locking zones (shaded regions) irregular dynamics are found. V_{\max} , maximal volume; f , frequency.

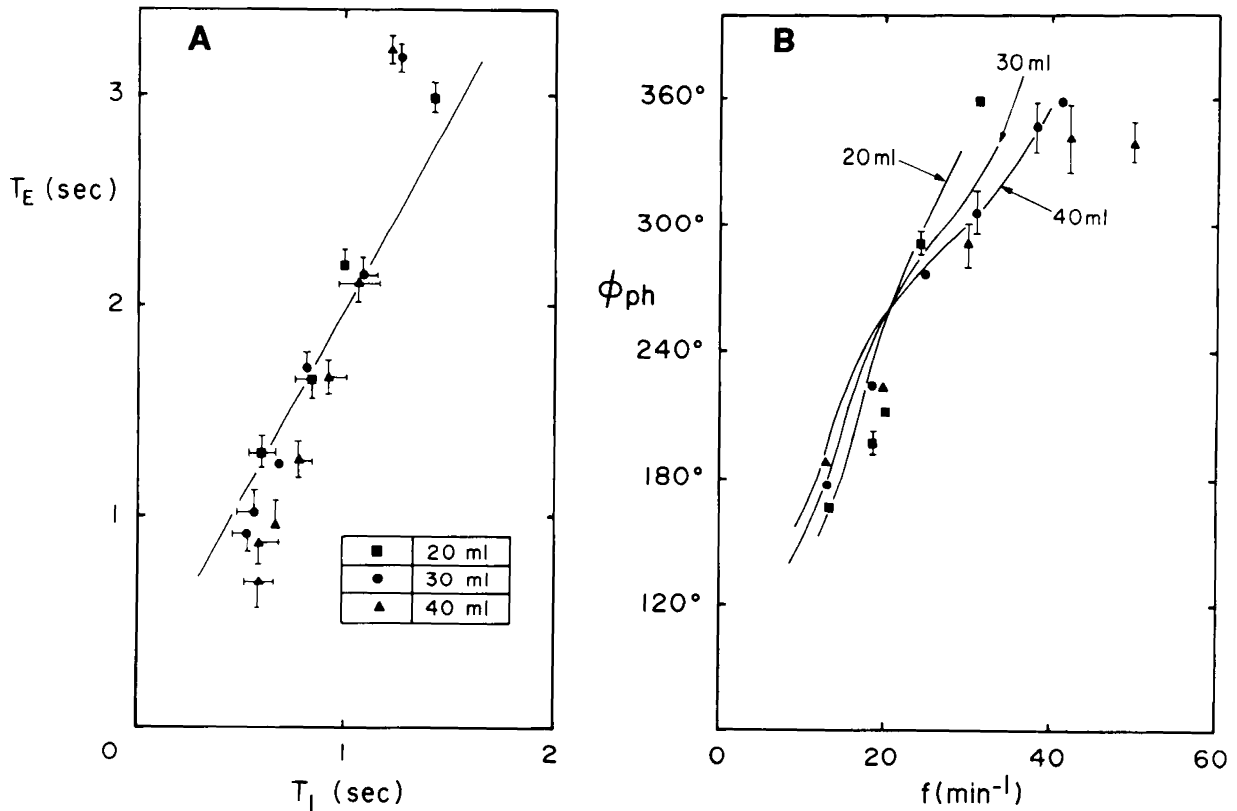


FIG. 3. Data from experimental studies (35) in 1:1 phase-locking zones. *A*: expiratory time (T_E) vs. inspiratory time (T_I); *B*: phase angle of phrenic zone taken over several frequencies and volumes of mechanical ventilator. *Superposed lines* show results from model (section III).

atory time (T_E) vs. inspiratory time (T_I); *B*: phase angle of phrenic onset, as defined in text, as function of frequency (f).

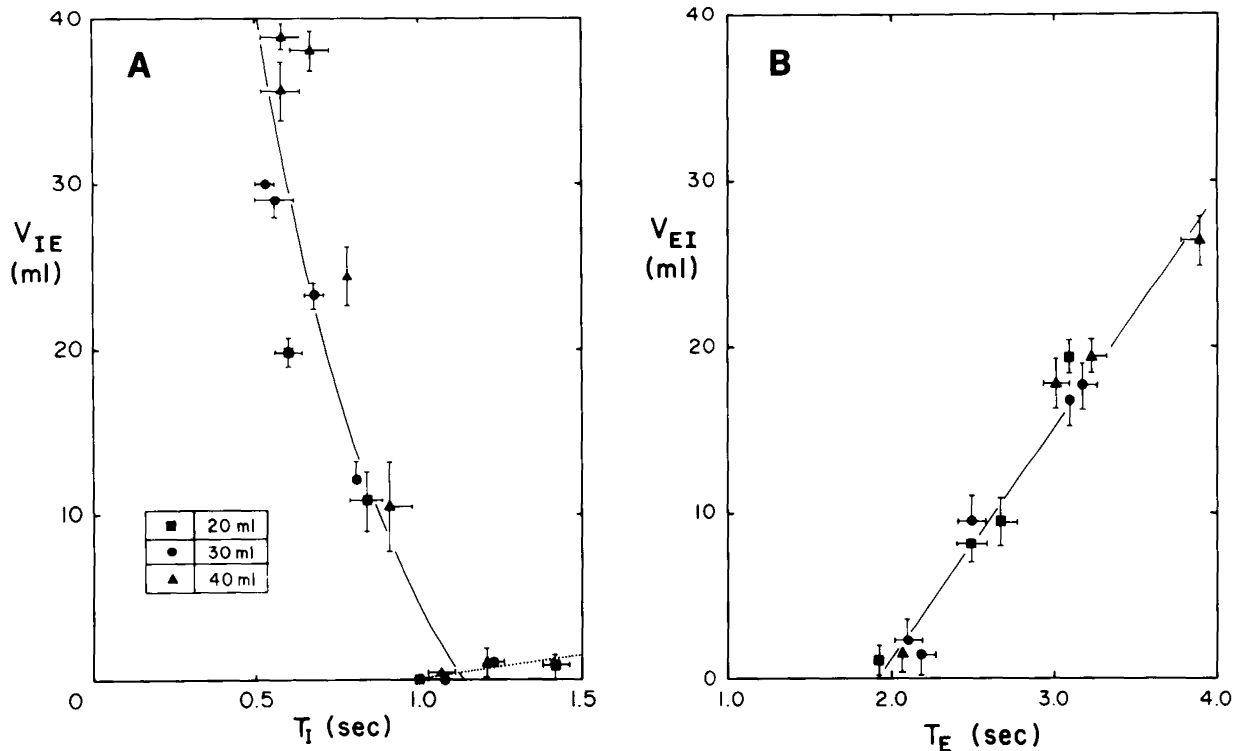


FIG. 4. Data from experimental studies (35) in 1:1 phase-locking zones. *A*: lung volume at end of inspiration (V_{IE}), as function of inspiratory time (T_I). *Solid curve* is hyperbolic fit to data for $f \geq f_{ph}$, where f_{ph} is intrinsic respiratory frequency ($V_{IE} = 37.6/T_I - 33.1$). *B*:

lung volume at 0.2 s before end of expiration (V_{EI}), as function of expiratory time (T_E) with $f \leq f_{ph}$. *Solid line*, linear fit to data ($V_{EI} = 13.9 T_E - 27.8$).

the phase of the phrenic onset relative to the ventilator cycle. The phase of the ventilator cycle is normalized to 360° , if we take the start of the ventilator cycle as 0° .

Figure 3*B* shows the phase of onset of the phrenic burst as f is varied. In Fig. 3 the superposed lines represent the properties of the model (see section III). Figure 4*A* shows

the lung volume at the end of the inspiratory phase (VIE) as a function of T_I obtained as ventilator frequency and volume are varied. For ventilator frequencies higher than the intrinsic frequency, the data were fit to a hyperbola. Figure 4B shows the lung volume 0.2 s before the start of inspiration (VEI) for ventilator frequencies less than the intrinsic frequency. Figure 4, A and B, taken together with Fig. 1, is used to set the parameters in the theoretical model (see section II). Once these parameters are set and the ventilator profiles are known, the complete dynamics for all frequencies and amplitudes of the ventilator can be theoretically computed. We now describe the theoretical model and give its main properties.

II. A MODEL FOR THE HERING-BREUER REFLEXES

The model is shown schematically in Fig. 5, and the main equations of the model are given in Table 1. We first give a brief overview of the model and then discuss the assumptions underlying the timing of T_I and T_E.

We assume that T_I is determined by the time required for an increasing inspiratory activity, which is analogous to "integrated" phrenic activity, to reach an inspiratory off-switch threshold and that T_E is determined by the time required for a decreasing expiratory activity to reach

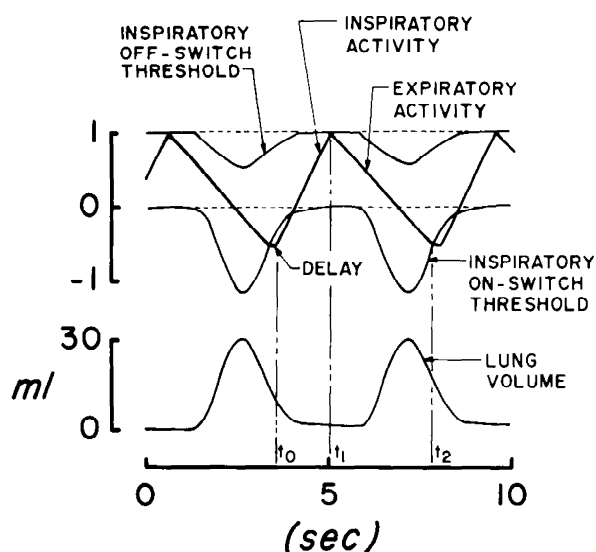


FIG. 5. Representation of model for respiratory phase locking with ventilator frequency of 13.5 min^{-1} and ventilator volume of 30 ml, using equations shown in Table 1 (intrinsic respiratory frequency equals 20 min^{-1}). In absence of lung inflation, inspiratory on-switch and off-switch thresholds would be constant as indicated by dashed lines. Lung inflation (lower trace) decreases thresholds, thereby giving Hering-Breuer reflexes. Times t_0 , t_1 , and t_2 correspond to notation in text and Table 1.

TABLE 1. Summary of model

Functions	Equation	Parameter Values
Inspiratory activity (Eq. 2)	$I(t) = I(t_0) + \alpha_I(t - t_0)$	$\alpha_I = 1.0 \text{ s}^{-1}$
Expiratory activity (Eq. 7)	$E(t) = E(t_1) - \alpha_E(t - t_1)$	$\alpha_E = 0.56 \text{ s}^{-1}$
Delay time		$\delta = 0.20 \text{ s}$
Inspiratory off-switch threshold (Eqs. 1 and 4)	$\theta_I(t) = k_I - \frac{\beta_I V(t)}{1 + (\beta_I/k_I)V(t)}$	$k_I = 1.0; \beta_I = 0.03 \text{ ml}^{-1}$
Inspiratory on-switch threshold (Eqs. 9 and 12)	$\theta_E(t) = k_E - \beta_E V(t)$	$k_E = 0.0; \beta_E = 0.040 \text{ ml}^{-1}$

a second lower threshold, the inspiratory on-switch threshold (Fig. 5) (3, 4, 7, 10, 24, 27, 36). The modulation of the thresholds leads to the Hering-Breuer reflexes. Starting with inspiratory activity equal to zero at any phase of the mechanical ventilator cycle, the model can be simulated on a digital computer, iteratively determining the subsequent durations of each inspiratory and expiratory phase. In contrast to a spontaneously breathing animal, in which lung inflation is coincident with phrenic (inspiratory) activity, in this model and in the experiments, the phase of inspiratory activity with respect to the ventilator cycle depends on the frequency and volume of the ventilator.

Timing of inspiration. As a dynamical model for the timing of inspiration we shall follow assumptions made by previous workers in which the termination of inspiration occurs by an "off-switch" mechanism (3, 4, 7, 10, 24, 27, 36). During the course of inspiration we assume that there is a centrally generated inspiratory activity $I(t)$, which increases linearly with time and is abruptly and discontinuously terminated on reaching a threshold $\theta_I(t)$. There are two components of $\theta_I(t)$. The first is a steady-state component k_I , associated with the long-term control of inspiratory cutoff by parameters such as CO_2 partial pressure (PCO_2), temperature, and the level of anesthesia. The second is a phasic component, $f_I(t)$, associated with the breath-by-breath control of inspiratory cutoff and originating from vagally mediated feedback due to periodic mechanical ventilation

$$\theta_I(t) = k_I - f_I(t) \quad (1)$$

If $t = t_0$ represents the onset of inspiration and $I(t_0)$ represents the level of inspiratory activity at $t = t_0$, then

$$I(t) = I(t_0) + \alpha_I(t - t_0) \quad (2)$$

where α_I is a positive constant. Inspiration is terminated when $I(t) = \theta_I(t)$, or

$$k_I = I(t) + f_I(t) \quad (3)$$

The above formulation is supported by previous work which suggests that an intrinsically generated central inspiratory activity and the pulmonary stretch receptor activity combine to cause the sudden activation of an inspiratory off-switch mechanism, on reaching a certain critical threshold (4).

In the following we assume that $f_I(t)$ is given by

$$f_I(t) = \frac{\beta_I V(t)}{1 + (\beta_I/k_I)V(t)} \quad (4)$$

where β_I is a constant. With this relation there is a nonlinear decrease of the inspiratory off-switch thresh-

old as volume increases so that the threshold (*Eq. 1*) never becomes negative. As well, this particular functional form for $f_I(t)$ gives a hyperbolic relationship between VIE and TI for high ventilation frequencies in the 1:1 zone.

To derive the VIE-TI relationship, let $t = t_1$ represent the time at which inspiration is terminated. Then, from *Eqs. 2-4* we obtain

$$I(t_0) + \alpha_I(t_1 - t_0) = k_I - \frac{\beta_I V(t_1)}{1 + (\beta_I/k_I)V(t_1)} \quad (5)$$

After rearranging terms and replacing $V(t_1)$ and $(t_1 - t_0)$ with the equivalent expressions VIE and TI, respectively, we obtain

$$\left(VIE + \frac{k_I}{\beta_I} \right) \left(TI + \frac{I(t_0)}{\alpha_I} \right) = \frac{k_I^2}{\alpha_I \beta_I} \quad (6)$$

Although it is generally agreed that the end-inspiratory volume-TI relationship is a monotonically decreasing curve, there is considerable controversy concerning the details of its shape (4, 7, 14, 22). The parametrization in this paper facilitates computations, but other choices are possible. In 1:1 phase locking at high frequencies, when the inspiratory inhibitory reflexes are important, $I(t_0) \simeq 0$ and *Eq. 6* is a hyperbola in agreement with Clark and von Euler (7).

The preceding analysis for the timing of inspiration accounts for the observation that lung inflations that occur during the inspiratory phase tend to shorten the duration of inspiration. In the present model we have assumed that the phasic component associated with the termination of inspiration is a function of the instantaneous lung volume. The timing of inspiration depends on other parameters such as inflation flow rate and waveform, pressure, and integrative central signal processing of afferent input (11, 12, 14, 27, 28, 31, 42). The present assumptions are thus approximations.

Timing of expiration. Although it is known that the duration of the expiratory phase is influenced by a variety of central and peripheral factors, the underlying mechanisms are not well understood (27, 43). It has been proposed (3, 4, 7, 10, 24, 27, 36) that expiration is timed by a central decaying expiratory activity, which we call $E(t)$. Assume that at end inspiration $E(t_1) = I(t_1)$ and that $E(t)$ decays linearly with time, so that

$$E(t) = E(t_1) - \alpha_E(t - t_1) \quad (7)$$

where α_E is a constant. Activity $E(t)$ ceases its decay on reaching a threshold $\theta_E(t)$. The assumptions we make with respect to $\theta_E(t)$ follow closely those described for $\theta_I(t)$. Thus $\theta_E(t)$ consists of a steady-state component k_E , which is modulated by a phasic component $f_E(t)$, so that

$$\theta_E(t) = k_E - f_E(t) \quad (8)$$

Expiratory activity reaches the threshold when $E(t) = \theta_E(t)$, or

$$E(t) = k_E - f_E(t) \quad (9)$$

Let $t = t_2$ represent the time when $E(t) = \theta_E$. We also assume a delay (δ) as part of the expiratory phase. The inclusion of this delay is justified by experiments in

which lung volume manipulations during the last 30% of the expiratory phase have little effect on the duration of expiration (27). Thus the expiratory phase is terminated at $t = t_2 + \delta$ with $E(t_2 + \delta) = E(t_2)$ and $TE = (t_2 - t_1) + \delta$. Then, from *Eqs. 2* and *7* we obtain

$$E(t_2) = I(t_0) + \alpha_I(t_1 - t_0) - \alpha_E(t_2 - t_1) \quad (10)$$

If we replace $(t_1 - t_0)$ with TI and $(t_2 - t_1)$ with $(TE - \delta)$ and note that in 1:1 phase locking $E(t_2) = I(t_0)$, we obtain the linear relation

$$TE = \left(\frac{\alpha_I}{\alpha_E} \right) TI + \delta \quad (11)$$

The phasic component of the inspiratory on-switch threshold associated with the timing of expiration, $f_E(t)$, is assumed to be proportional to lung volume $V(t)$, so that

$$f_E(t) = \beta_E V(t) \quad (12)$$

where β_E is a constant of proportionality. From *Eqs. 7, 9, and 12*, with $t = t_2$

$$E(t_1) - \alpha_E(t_2 - t_1) = k_E - \beta_E V(t_2) \quad (13)$$

If we replace $(t_2 - t_1)$ with $(TE - \delta)$, call $VEI = V(t_2)$, and rearrange terms, *Eq. 13* yields

$$VEI = \frac{\alpha_E}{\beta_E} TE + \frac{k_E - \alpha_E \delta - E(t_1)}{\beta_E} \quad (14)$$

Determination of parameters of the model. The body of experimental data is large, and parameters are comparatively few. Consequently the parameters can be set in different ways by selecting different subsets of the data. In the course of developing the model we have tried different methods of parameter determination. In general, parameters determined using different methods did not vary more than about 10-20%. Although we have not carried out a systematic study of the sensitivity of the model to parameter variation, we have performed several simulations of the model using different sets of parameters. These simulations showed that the main properties of the model, which we will describe below, are not sensitive to comparatively small (on the order of 10-20%) variations in the parameters of the model.

For a given set of experimental conditions (constant blood gases, temperature, anesthesia), the threshold parameters k_I and k_E are expected to remain constant. We arbitrarily select the values $k_I = 1.0$ and $k_E = 0.0$.

With the ventilator shut off we measure $TI = 1.0$ s and $TE = 2.0$ s (*Fig. 1*). Since inspiration is timed by the linearly increasing inspiratory activity, from *Eqs. 2* and *3* we obtain

$$\alpha_I = \frac{1.0}{TI} = 1.0 \text{ s}^{-1} \quad (15)$$

To determine α_E we will assume $\delta = 0.2$ s, which is in the range found by previous workers (27). From *Eq. 13* with $E(t_1) = 1.0$, $V(t_2) = 0$, and $t_2 - t_1 = TE - \delta$, we obtain

$$\alpha_E = \frac{1.0}{TE - \delta} = 0.56 \text{ s}^{-1} \quad (16)$$

Note that α_I , α_E , and δ are also related through Eq. 11. The choice of parameters here does not agree with the values found by fitting Eq. 11 to the data in Fig. 3A. This discrepancy is discussed later.

The parameters in the inspiratory off-switch threshold can be determined by fitting the VIE-TI data to the hyperbola

$$(VIE - V_0)(TI - T_0) = C \quad (17)$$

A linear regression of VIE vs. $1/(TI - T_0)$ was performed for different values of T_0 . The best fit ($r = 0.88$) was obtained for $T_0 = 0$, $V_0 = -33.1$ ml, and $C = 37.6$ ml s. As we have noted already, in the 1:1 zone when the Hering-Breuer inspiratory inhibitory reflexes are important $I(t_0) \approx 0$, in agreement with the value $T_0 = 0$ (see Eq. 6). By equating corresponding terms in Eqs. 6 and 17 we can now obtain two independent estimates for β_I

$$\beta_I = -\frac{k_I}{V_0} = 0.030 \text{ ml}^{-1} \quad (18a)$$

$$\beta_I = \frac{k_I^2}{\alpha_I C} = 0.027 \text{ ml}^{-1} \quad (18b)$$

Both estimates show close agreement. Numerical simulations were performed with $\beta_I = 0.030 \text{ ml}^{-1}$.

The parameters for the expiratory on-switch threshold can be determined by fitting the VEI-TE data to the line

$$VEI = ATE + B \quad (19)$$

An excellent ($r = 0.98$) fit to the data was obtained for

$A = 13.9 \text{ ml} \cdot \text{s}^{-1}$ and $B = -27.8 \text{ ml}$. By equating corresponding terms in Eqs. 14 and 19 we can obtain two independent estimates for β_E , if we assume $\alpha_E = 0.56 \text{ s}^{-1}$, $k_E = 0$, $\delta = 0.2 \text{ s}$, and $E(t_1) \approx 1.0$

$$\beta_E = \frac{A}{\alpha_E} = 0.040 \text{ ml}^{-1} \quad (20a)$$

$$\beta_E = \frac{k_E - \alpha_E \delta - E(t_1)}{B} = 0.040 \text{ ml}^{-1} \quad (20b)$$

III. PROPERTIES OF THE MODEL

We now consider the properties of the model as a function of volume magnitude, V_{\max} , and frequency, f , of the periodic input $V(t)$. The periodic volume input $V(t)$, is approximated as a piecewise linear function interpolated from digitized measurements at 100 points of the mechanical ventilation cycle for $V_{\max} = 30 \text{ ml}$ and $f = 30 \text{ min}^{-1}$. Periodic inputs with different values of V_{\max} and f were obtained by linear scaling of the digitized volume with $V_{\max} = 30 \text{ ml}$ and $f = 30 \text{ min}^{-1}$. The system was numerically simulated for approximately 200 combinations of V_{\max} and f in the range $V_{\max} = 2 - 50 \text{ ml}$ and $f = 5 - 60 \text{ min}^{-1}$, using the parameters determined in section II. The usual circumstance was that a stable dynamics was reached after a number of iterations.

The main results of the numerical simulations are contained in Fig. 6 (cf. Fig. 2). Although the volume threshold parameters in the 1:1 region derived from Fig. 4 were utilized in the simulations, these parameters also

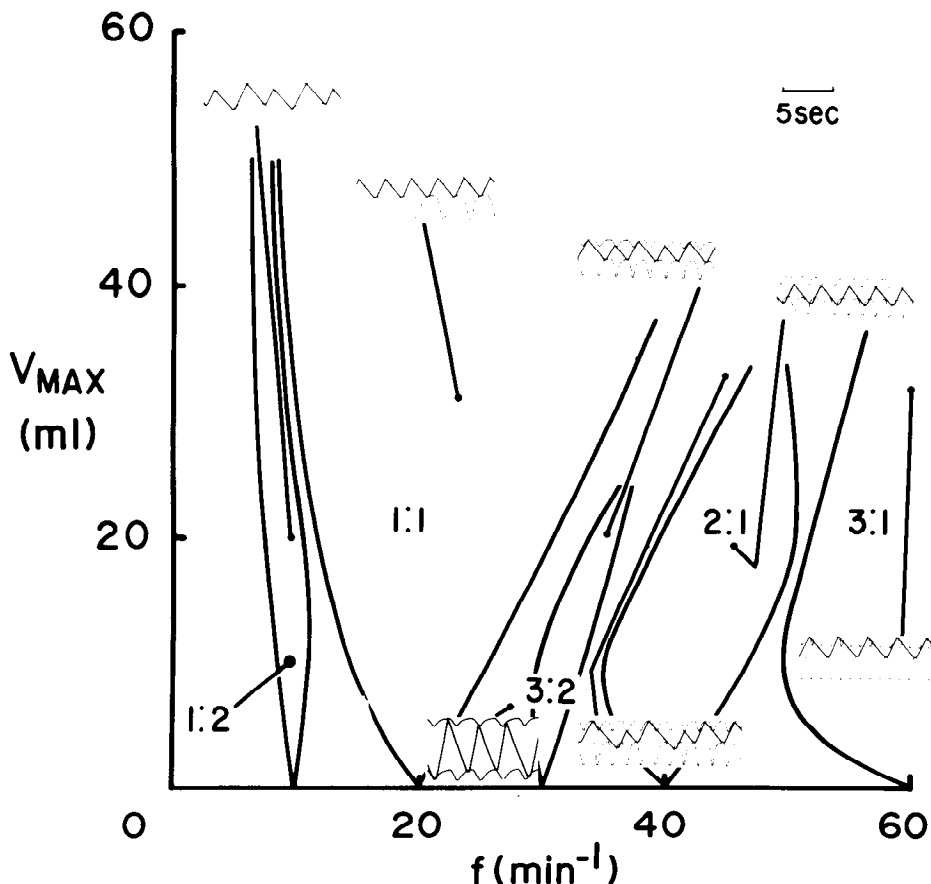


FIG. 6. Composite showing schematic diagram of different phase-locking zones obtained from model and representative traces of dynamics in each zone. In each inset, same format of Fig. 5 is used, but since ventilator volume trace is directly reflected in oscillating thresholds, it is not included. Scale is the same for all insets. Irregular dynamics between 3:2 and 2:1 zone was found when "noise" was added to model (see text).

give a very good agreement with the dynamics observed outside this region. In particular, the following correspondences are found: 1) the dominant phase-locking patterns are 1:2, 1:1, 3:2, 2:1, and 3:1; 2) these patterns occur for characteristic values of V_{\max} and f in the model and experimental system; 3) high-amplitude inspiratory bursts are terminated at maximum threshold levels where the periodic volume input is approximately zero, whereas low-amplitude inspiratory bursts are terminated prematurely by the periodic volume input; and 4) the non-phase-locked dynamics at low volumes found in the model system are similar to the dynamics found in the experimental system at low volumes. Such rhythms, in which there is a continued shifting of phase between the two rhythms are often called quasiperiodic (17).

In addition to these correspondences between theory and experiment, there are also discrepancies. We briefly describe several of these discrepancies and comment on their possible origin.

1) For inflation volumes above 10 ml, the model generally does not show irregular dynamics, whereas irregular dynamics are often observed in the experimental system (35). One possible source of irregularities in the experiment is "noise" that may arise as a result of fluctuations of brain stem neural activity or in afferent input to the brain stem (17). One way to account for noise is to add small stochastic terms to the times at which the thresholds are reached and to iterate the system with these perturbed times (17). When this is carried out, irregular rhythms such as those observed in the experimental system are found. The irregular rhythm in Fig. 6 lying between the 2:1 and 3:2 zones was generated with added noise in the model and is similar to the experimentally observed pattern (Fig. 2). In general, addition of noise gives zones of irregular dynamics between the major zones shown in Fig. 6 (17, 34).

2) The theoretical model predicts many other phase-locking zones at volumes above 10 ml. These zones are not shown in Fig. 6, since they occupy comparatively small regions in the parameter space. Some of the patterns in these zones (4:3 and 5:2) have been observed on occasion in the experiment (34, 35), whereas other zones (e.g., 5:3, 4:2, and 11:9) have not been observed experimentally. One possible reason for nonobservation of theoretically predicted zones is that they will be destroyed by noise (17, 34). Some of these patterns may be observed if the appropriate regions of parameter space are explored sufficiently carefully. For example, at comparatively high volumes and frequencies ($V_{\max} = 40$, $f = 45$), one expects to see a 4:2 rhythm, but extensive experimental studies were not carried out in this region of parameter space. On theoretical grounds we expect that the "fine structure" of the phase-locking zones will be quite complex and consequently difficult to observe experimentally (17, 19, 29).

3) In the 1:1 zone, although both the model and experiment show linear relation between TE and TI (Fig. 3A), there is not good quantitative agreement. A least-squares fit to the experimental data gives $TE = 2.8TI - 0.72$ ($r = 0.96$), whereas, if we use the parameters in Table 1, Eq. 11 gives $TE = 1.8TI + 0.2$. Different choices of parameters could have been made to give better agree-

ment with the data in Fig. 3A, but such manipulations were not systematically explored. The lack of agreement may well reflect deficiencies in the model. If $E(t)$ were exponentially decreasing (in accord with Refs. 3, 4, 7, 10, 24, and 27), we expect that this would lead to a prolongation of TE relative to TI at low ventilation frequencies (high values of TE and TI in Fig. 3A). As well, flow effects (11, 12, 14) should be important for high ventilation frequencies (low values of TI in Fig. 3A). Flow effects may also be playing a role in the discrepancies in the phase angle between theory and experiment at ventilation volumes of 40 ml at the higher frequencies (Fig. 3B).

IV. DISCUSSION

The simple mathematical model in section II gives good agreement with experiments on mechanical ventilation of anesthetized, paralyzed cats. Although the mathematical model was based on previous experimental and theoretical studies, many modifications were made to simplify previous models to facilitate numerical computations and determination of parameters. The main novel feature of the model is the incorporation of two oscillating thresholds to represent the phasic afferent activity. Previous workers either used one oscillating threshold or incorporated the effects of lung inflation by a direct change in inspiratory and expiratory activities (3, 4, 7, 10, 24, 27, 36). Models with two oscillating thresholds can be shown to have a close correspondence with nonlinear equations based on the van der Pol oscillator (see APPENDIX). Models with two oscillating thresholds are also appropriate in other examples of periodic forcing of nonlinear oscillators (38).

Modifications could be made to make the model more realistic. For example, such modifications would necessarily include the effects of flow and pressure on pulmonary afferent activity and the central processing of vagal activity (11, 12, 14, 27, 28, 31, 42, 43). In the context of the mathematical model, such changes could be incorporated by changing the threshold functions, $f_I(t)$ and $f_E(t)$.

There are three main reasons why we have not attempted to incorporate these additional factors. 1) There is not now general agreement about the relative importance of these factors. 2) Inclusion of additional factors would enormously complicate the mathematical formulation. For example, models of central processing of vagal input in idealized situations alone incorporate four to six parameters (43). 3) Even if additional factors were included it is unlikely that they would change the main qualitative features of the model. As we have already noted, the properties of the model are quite insensitive to small parametric changes.

Although there are not large qualitative differences with modifications of the model, some quantitative differences can be observed. For example, if the VIE-TI curve is fit to a straight line for $f \geq f_{ph}$ one observes an overly strong inspiratory inhibitory reflex, and as a consequence 1:1 entrainment in the model at high ventilator volumes occurs at higher frequencies than is actually observed experimentally. Also, by taking δ (the delay time) to be zero, one observes a downward shift in the

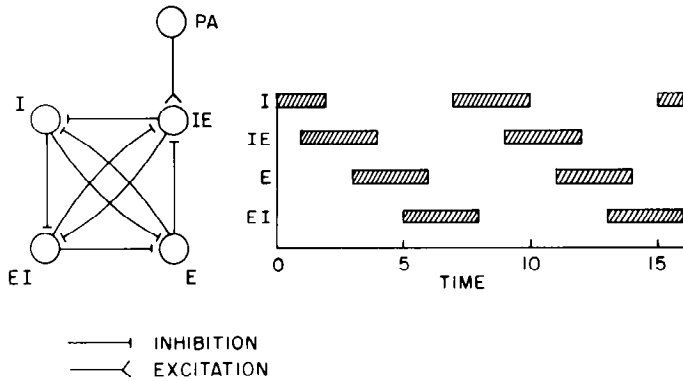


FIG. 7. Model for interconnections between brain stem respiratory neurons and associated firing activity patterns. Four pools of neurons I, IE, E, and EI correspond to inspiratory, inspiratory-expiratory, expiratory, and expiratory-inspiratory pools, respectively, described by Cohen (8, 9). Each of these 4 pools is also assumed to receive tonic excitatory inputs (not shown) that will lead to tonic firing in absence of network interactions. Pulmonary afferents (PA) are activated during lung inflation, leading to Hering-Breuer reflexes. Format adopted from Refs. 21 and 26.

phase angles in Fig. 3B.

We believe that the above model for the effects of pulmonary afferents on central respiratory activity does capture, albeit in a highly oversimplified way, salient aspects of the real physiological situation. Consequently it is reasonable to try to understand the connection between this model and more detailed models, based on the neurophysiology of respiratory rhythmogenesis. Since respiratory-related neural activity in the brain stem is not yet well understood, formulation of detailed models is necessarily speculative (19). The following model for the respiratory oscillator is offered to give a qualitative picture of how the model we have presented might be generated by a neural network.

In Fig. 7 we display a network model for respiratory rhythmogenesis. There are four pools of neurons, corresponding to the inspiratory (I), expiratory (E), and phase-spanning (IE and EI) neurons described by Cohen (8, 9). There are inhibitory synaptic connections between some of these pools. Each pool of neurons is also assumed to receive tonic excitatory input, for example, from CO_2 -sensitive neurons, and may have excitatory inputs from other members of the same pool (6). The tonic input is sufficiently strong to result in firing in the absence of inhibitory input from other neurons in the network. However, the presence of the inhibitory interactions lead to a cyclic firing pattern (Fig. 7). The time during which each neuronal pool fires above some critical firing frequency is indicated by a shaded bar. Note that the firing pattern corresponds to the schematic diagram in the article by Cohen (8, p. 17). This network was originally proposed as a model for controlling limb movements in *Urodela* [(26, 40); for detailed quantitative studies of this model, see (18, 21); for different network models for respiratory rhythmogenesis and reviews of earlier literature, see (13a, 16)].

The Hering-Breuer reflexes can be accounted for by assuming that the pulmonary afferents project to the IE pool (this has the same function as the I_s pool described in Refs. 8-10) by excitatory synapses. Consequently

excitation of the IE neurons leads to an inhibition of the I neurons leading to the Hering-Breuer inspiratory-inhibitory reflex. Excitation of the IE neurons will also lead to a facilitation of expiration (Hering-Breuer expiratory-promoting reflex), because the resulting inhibition of the I and EI pools will in turn lead to less inhibition of the E pools (i.e., there will be disinhibition of the E pool activity). Since the effects of lung inflation on expiration have to pass through three synapses and through two separate pathways, it is reasonable to expect that these effects will be more complex and show "integration" and time delays, compared with the effects of lung inflation on inspiratory timing (27, 43).

The model depicted in Fig. 7 is an extension of the mechanism proposed by Salmoiraghi and Burns (6, 37) for respiratory rhythmogenesis. In both models there are mutually inhibitory interconnections between the I and E pools. Because of this common feature, some criticisms of the Salmoiraghi and Burns model are also applicable to the model in Fig. 7. Thus, as suggested by Merrill (30), the E and I pools might be further subdivided into functionally distinct classes. In the model in Fig. 7, phase switching occurs as a consequence of network interactions and does not require additional features such as pacemaker cells, fatigue, or accumulating refractoriness (9, 21). Differential equations that represent the neural model in Fig. 7 have been developed and display stable limit-cycle oscillations (18). Since these mathematical models employ thresholds it should be possible, by judicious choice of parameters, to bring the network model in Fig. 7 into at least rough correspondence with the models described in this paper. However, since analysis of the resulting equations, particularly under periodic forcing, is not easy, and the network model in Fig. 7 is speculative, further work along these lines has not been carried out.

Although respiratory entrainment by a mechanical ventilator is a complex phenomenon, the mathematical model for the Hering-Breuer reflexes presented here gives good agreement with the experiment. Thus the analysis of phase-locking data can be used to derive data about the Hering-Breuer reflexes. Since mechanical ventilation of humans is often performed clinically, analysis of respiratory entrainment in humans will provide a new technique for analysis of human Hering-Breuer reflexes. Such information should be of use in the efficient utilization of mechanical ventilators in the clinic.

APPENDIX

Here we explicitly demonstrate that a transformation of the van der Pol equations can give a system of equations that has a close correspondence with the theoretical model derived in section II. This correspondence is of interest, since some authors have considered periodically forced van der Pol equations (appropriately modified) as a model for respiratory rhythmogenesis and phase locking (2, 3, 15). The discussion is directed toward mathematically inclined readers and assumes a familiarity with standard methods of phase plane analysis of the van der Pol equation (25).

The periodically forced van der Pol equation is generally written (29)

$$\frac{dy}{dt} = -\epsilon x + p(t) \quad (A1a)$$

$$\frac{dx}{dt} = \frac{1}{\epsilon} [y - \Phi(x)] \tag{A1b}$$

where x and y are the state variables, $p(t)$ is a periodic function of time (the forcing function), ϵ is a positive constant which is often taken to be small, and $\Phi(x)$ is a nonlinear function [$\Phi(x) = x^3/3 - x$ in the case initially considered by van der Pol]. If we assume

$$p(t) = \frac{dq(t)}{dt} \tag{A2a}$$

$$u(t) = y(t) - q(t) \tag{A2b}$$

Eq. A1 can be transformed to yield

$$\frac{du}{dt} = -\epsilon x \tag{A3a}$$

$$\frac{dx}{dt} = \frac{1}{\epsilon} [\mu - \Phi(x) + q(t)] \tag{A3b}$$

To draw the analogy with the theoretical model in section II, we will associate the variable u in Eq. A2 with both the inspiratory and expiratory activities. Since these activities are linear functions of time in the model, but are nonlinear in Eq. A2, modifications are needed. Define the Heaviside function

$$\begin{aligned} H(x) &= 0, & x < 0 \\ H(x) &= 1, & 0 \leq x \end{aligned} \tag{A4}$$

and the piecewise linear function $\Phi_{PL}(x)$

$$\begin{aligned} \Phi_{PL}(x) &= \frac{x}{2} + \frac{3}{2} & \text{for } x < -1 \\ \Phi_{PL}(x) &= \frac{-x}{2} + \frac{1}{2} & \text{for } -1 \leq x \leq 1 \\ \Phi_{PL}(x) &= \frac{x}{2} - \frac{1}{2} & \text{for } x > 1 \end{aligned} \tag{A5}$$

Now consider the transformed equations

$$\frac{du}{dt} = \alpha[1 - 2H(x)] \tag{A6a}$$

$$\frac{dx}{dt} = \frac{1}{\epsilon} [u - \Phi_{PL}(x) + q(t)] \tag{A6b}$$

The (u, x) phase plane for Eq. A6 with $q(t) = 0$ is shown in Fig. 8A. The heavy lines give the piecewise linear function in Eq. A5. In the limit of small ϵ and with $q(t) = 0$ there is a slow rise along the left-hand branch, a rapid shift to the right-hand branch initiated when $u = 1$, a slow decline following the right-hand branch to $u = 0$, and then a rapid shift to the left-hand branch at $u = 0$ (Fig. 8A). By taking ϵ sufficiently close to zero, the time spent on the fast parts of the cycle (dashed lines in Fig. 8A) can be made arbitrarily small. In this case the plot of u as a function of time is given in Fig. 8B for $\alpha = 1$.

Periodic forcing in Eq. A6 can now be given a simple geometric interpretation. Assume $q(t) = 0.3 \sin 2\pi t$. When $du/dt > 0$, switching from the left-hand branch to the right-hand branch is initiated when $u(t) = 1 + 0.3 \sin 2\pi t$, and when $du/dt < 0$, the switching from the right-hand branch to the left-hand branch is initiated when $u(t) = 0.3 \sin 2\pi t$. Thus for Eq. A6 there is a linear rising and falling to the oscillating "thresholds" (Fig. 8C). To complete the correspondence with the model in section II it is necessary to incorporate 1) different rates of rise and fall of $u(t)$ and 2) different threshold switching functions. By manipulating the Heaviside function, different functions can be taken in the left- and right-half planes of Fig. 8A. Consider the nonlinear equation

$$\frac{du}{dt} = \alpha_I - (\alpha_I + \alpha_E)H(x) \tag{A7a}$$

$$\frac{dx}{dt} = \frac{1}{\epsilon} \{u - \Phi_{PL}(x) - f_I(t) + [f_I(t) - f_E(t)]H(x)\} \tag{A7b}$$

where α_I , α_E , $f_I(t)$, and $f_E(t)$ are as defined in section II (with $k_I = 1$ and $k_E = 0.0$) and $0 < \epsilon \ll 1$. In the left-hand plane u increases linearly

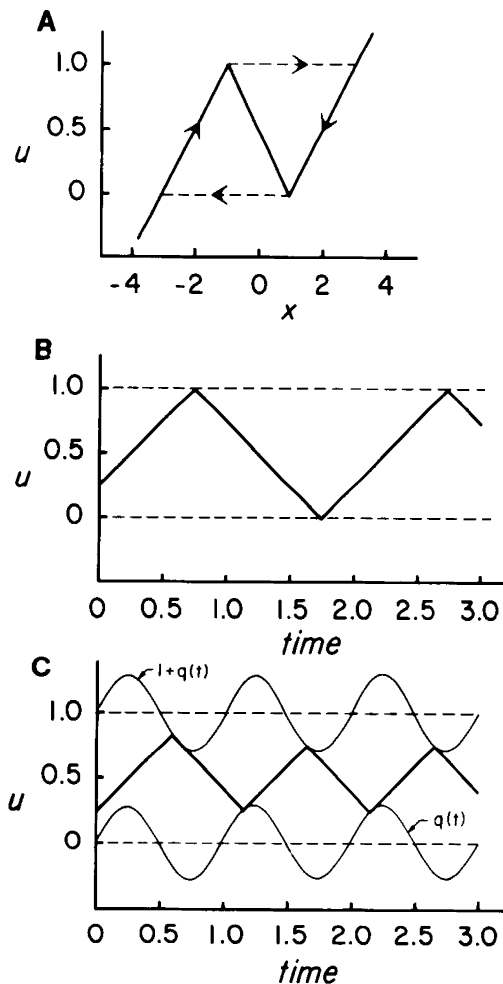


FIG. 8. A: phase plane representation of oscillator given in Eq. A6. Piecewise linear function (Eq. A5) is represented by heavy lines. Arrows show cycle when $0 < \epsilon \ll 1$. In this limit, dashed lines represent fast transitions between different branches of piecewise linear function. B: dynamics in Eq. A6 for $q(t) = 0$ and $\alpha = 1$. There is an oscillation with a period of 2 time units. C: dynamics in Eq. A6 for $q(t) = 0.3 \sin 2\pi t$ and $\alpha = 1$. There is 1:1 entrainment, even though intrinsic frequency of oscillator is one-half the frequency of periodic forcing.

with a slope α_I . Thus u in the left-hand plane corresponds to $I(t)$. There is a rapid switch to the right-hand branch of Eq. A5 which is initiated when Eq. 3 is satisfied. In the right-half plane, $u(t)$ decreases with a slope α_E and corresponds to $E(t)$. A switch to the left-hand branch of Eq. A5 is initiated when Eq. 9 holds. The only parameter not included in the nonlinear model is the delay time δ , which in the limit-cycle model corresponds to the time it takes to cross from the right-hand branch to the left-hand branch of Eq. A5. This time will be a short but finite time for nonzero values of ϵ . In the limit-cycle model, note, however, that there are equivalent delays between the inspiratory and expiratory phases and between the expiratory and inspiratory phases. Since this is not the case in the model in section II, there is close but not exact correspondence between Eq. A7 and the model in section II. In general, for finite values of ϵ there are also differences in the topological properties of the limit-cycle model and the discrete model in section II. These differences are reflected in the effects of single stimuli in resetting the rhythm (20).

We thank Dr. T. Trippenbach for help with the experimental studies and for many useful discussions.

This research has been supported by grants from the Natural Sciences and Engineering Research Council and the Canadian Lung Association. G. A. Petrillo was a recipient of a fellowship from the Conseil de la Recherche en Santé du Québec.

Address reprint requests to L. Glass.

Received 3 May 1983; accepted in final form 20 October 1983.

REFERENCES

1. ADRIAN, E. D. Afferent impulses in the vagus and their effects on respiration. *J. Physiol. London* 79: 322-358, 1933.
2. BACONNIER, P. G., G. BENCHETRIT, J. DEMONGEOT, AND T. PHAM DINH. Etude des phénomènes d'entraînement: application au système respiratoire. In: *Actes du Premier Séminaire de l'École de Biologie Théorique*, edited by H. Le Guyader and T. Moulin. Paris: Ecole Nationale de Technique Avancées, 1982, p. 483-503.
3. BACONNIER, P., G. BENCHETRIT, J. DEMONGEOT, AND T. PHAM DINH. Simulation of the entrainment of the respiratory rhythm by two conceptually different models. *Lect. Notes Biomath.* 49: 2-16, 1983.
4. BRADLEY, G. W., C. VON EULER, I. MARTILLA, AND B. ROOS. A model of the central and reflex inhibition of inspiration in the cat. *Biol. Cybern.* 19: 105-116, 1975.
5. BREUER, J. Die Selbststeuerung der Atmung durch den Nervus Vagus. *Sbev. Akad. Wiss. Wien.* 58: 909-937, 1968. (English translation by E. Ullman. In: *Breathing: Hering-Breuer Centenary Symposium*, edited by R. Porter. London: Churchill, 1970, p. 365-394.)
6. BURNS, B. D., AND G. C. SALMOIRAGHI. Repetitive firing of respiratory neurones during their burst activity. *J. Neurophysiol.* 23: 27-46, 1960.
7. CLARK, F. J., AND C. VON EULER. On the regulation of depth and rate of breathing. *J. Physiol. London* 222: 267-295, 1972.
8. COHEN, M. I. The genesis of respiratory rhythmicity. In: *Central-Rhythmic and Regulation*, edited by W. Umbach and H. P. Koepchen. Stuttgart, W. Germany: Hippokrates, 1975, p. 15-35.
9. COHEN, M. I. Neurogenesis of respiratory rhythm in the animal. *Physiol. Rev.* 59: 1105-1173, 1979.
10. COHEN, M. I., AND J. L. FELDMAN. Models of respiratory phase switching. *Federation Proc.* 36: 2367-2374, 1977.
11. CROSS, B. A., P. W. JONES, AND A. GUZ. The role of vagal afferent information during inspiration in determining phrenic motoneurone output. *Respir. Physiol.* 39: 149-167, 1980.
12. DAVIS, H. L., S. F. WARD, AND E. H. LAMBERT. Effect of volume and rate of inflation and deflation on transpulmonary pressure and response of pulmonary stretch receptors. *Am. J. Physiol.* 187: 558-566, 1956.
13. FALLERT, M., AND R. MUHLEMANN. Der Hering-Breuer Reflex bei Kunstlicher Beatmung des Kaninchens. I. Die Auslösung der reflektorischen Inspirationen durch den Respiator. *Pfluegers Arch.* 330: 162-174, 1971.
- 13a. FELDMAN, J. L., AND J. D. COWAN. Large scale activity in neural nets. II. A model for the brainstem respiratory oscillator. *Biol. Cybern.* 17: 39-51, 1975.
14. FELDMAN, J. L., AND H. GAUTIER. Interaction of pulmonary afferents and pneumotoxic center in control of respiratory pattern in cats. *J. Neurophysiol.* 39: 31-44, 1976.
15. FINCHAM, W., AND C. LIASSIDES. The role of the van der Pol oscillator in the control of breathing in the human. In: *Proceedings of the UK Simulation Council Conference on Computer Simulation*. Surrey, UK: IPC Science and Technology Press, 1978.
16. GEMAN, S., AND M. MILLER. Computer simulation of brain stem respiratory activity. *J. Appl. Physiol.* 41: 931-938, 1976.
17. GLASS, L., C. GRAVES, G. A. PETRILLO, AND M. C. MACKEY. Unstable dynamics of a periodically driven oscillator in the presence of noise. *J. Theor. Biol.* 86: 455-475, 1980.
18. GLASS, L., AND J. S. PASTERNAK. Prediction of limit cycles in mathematical models of biological oscillations. *Bull. Math. Biol.* 40: 27-44, 1978.
19. GLASS, L., AND R. PEREZ. The fine structure of phase locking. *Phys. Rev. Lett.* 48: 1772-1775, 1982.
20. GLASS, L., AND A. T. WINFREE. Discontinuities in phase-resetting experiments. *Am. J. Physiol.* 246 (Regulatory Integrative Comp. Physiol. 15): R251-R258, 1984.
21. GLASS, L., AND R. E. YOUNG. Structure and dynamics of neural network oscillators. *Brain Res.* 179: 207-218, 1979.
22. GRUNSTEIN, M. M., M. YOUNES, AND J. MILIC-EMILI. Control of tidal volume and respiratory frequency in anesthetized cats. *J. Appl. Physiol.* 35: 463-476, 1973.
23. GUEVARA, M. R., L. GLASS, AND A. SHRIER. Phase locking, period-doubling bifurcations, and irregular dynamics in periodically stimulated cardiac cells. *Science* 214: 1350-1353, 1981.
24. HERCZYNSKI, R., AND W. KARCEWSKI. Neural control of breathing: a system analysis. *Acta Physiol. Pol.* 27: 109-130, 1976.
25. HIRSCH, M. W., AND S. SMALE. *Differential Equations, Dynamical Systems and Linear Algebra*. New York: Academic, 1974, chapt. 10.
26. KLING, V., AND G. SZEKELEY. Simulation of rhythmic nervous activities. I. Function of networks with cyclic inhibitions. *Kybernetik* 5: 89-103, 1968.
27. KNOX, C. K. Characteristics of inflation and deflation reflexes during expiration in the cat. *J. Neurophysiol.* 36: 284-295, 1973.
28. LARRABEE, M. G., AND R. HODES. Cyclic changes in the respiratory centers, revealed by the effects of afferent impulses. *Am. J. Physiol.* 155: 147-164, 1948.
29. LEVI, M. Qualitative analysis of the periodically forced relaxation oscillations. *Mem. Am. Math. Soc.* 244, 1981.
30. MERRILL, E. G. Where are the real respiratory neurons? *Federation Proc.* 40: 2389-2394, 1981.
31. MORTOLA, J. P., AND G. SANT'AMBROGIO. Mechanics of the trachea and behaviour of its slowly adapting stretch receptors. *J. Physiol. London* 286: 577-590, 1979.
32. MUHLEMANN, R., AND M. FALLERT. Der Hering-Breuer-Reflex bei Kunstlicher Beatmung des Kaninchens. II. Die Reflexunterbrechung durch schrittweise Vaguskuhling. *Pfluegers Arch.* 330: 175-188, 1971.
33. PERKEL, D. H., J. H. SCHULMAN, T. H. BULLOCK, G. P. MOORE, AND J. P. SEGUNDO. Pacemaker neurons: effects of regularly spaced synaptic input. *Science* 145: 61-63, 1964.
34. PETRILLO, G. A. *Phase Locking—a Dynamic Approach to the Study of Respiration* (PhD thesis). Montreal, Quebec, Canada: McGill Univ., 1981.
35. PETRILLO, G. A., L. GLASS, AND T. TRIPPENBACH. Phase locking of the respiratory rhythm in cats to a mechanical ventilator. *Can. J. Physiol. Pharmacol.* 61: 599-607, 1983.
36. REMMERS, J. E. Analysis of ventilatory response. *Chest* 70 Suppl. 1, 1976.
37. SALMOIRAGHI, G. C., AND B. D. BURNS. Notes on mechanism of rhythmic respiration. *J. Neurophysiol.* 23: 14-26, 1960.
38. SCHARSTEIN, H. Input-output relationship of the leaky-integrator neuron model. *J. Math. Biol.* 8: 403-420, 1979.
39. SEGUNDO, J. P. Pacemaker synaptic interactions: modelled locking and paradoxical features. *Biol. Cybern.* 35: 55-62, 1979.
40. SZEKELEY, G. Logical network for controlling limb movements in Urodela. *Acta Physiol. Hung.* 27: 285-289, 1965.
41. VIBERT, J.-F., D. CAILLE, AND J. P. SEGUNDO. Respiratory oscillator entrainment by periodic vagal afferents. *Biol. Cybern.* 41: 119-130, 1981.
42. YOUNES, M., AND J. POLACHEK. Temporal changes in effectiveness of a constant inspiratory terminating vagal stimulus. *J. Appl. Physiol.: Respirat. Environ. Exercise Physiol.* 45: 80-86, 1981.
43. ZUPERKU, E. J., F. A. HOPP, AND J. P. KAMPINE. Central integration of pulmonary stretch receptor input in the control of expiration. *J. Appl. Physiol.: Respirat. Environ. Exercise Physiol.* 52: 1296-1315, 1982.